Reis *et al. Chem. Biol. Technol. Agric.* (2024) 11:61
https://doi.org/10.1186/s40538-024-00586-w

Chemical and Biological Technologies in Agriculture

RESEARCH

Open Access

Changes in soil bacterial community structure in a short-term trial with different silicate rock powders

Betania Roqueto Reis[1], Ana Luisa Soares Vasconcelos[1], Antonio Marcos Miranda Silva[1], Fernando Dini Andreote[1] and Antonio Carlos Azevedo[1*]

Abstract

Background The use of rock powders in soil has emerged as a nature-based technology to improve soil properties relevant to crop development and for atmospheric carbon dioxide removal (CDR) via enhanced rock weathering (ERW). Although modeling this process is crucial, the soil microbiome has been identified as the main reason why several experimental and field results do not fit the geochemical and kinetic theoretical models. Here, the hypothesis that the bacterial community structure is modulated by the application of different silicate rock powders was tested. One phonolite, three basalt variations and one granite, as well as KCl treatments, were applied to a Ferralsol cultivated with *Brachiaria* in short-term pedogeochemical experiments and assessed after 1 (1M), 4 (4M) and 8 (8M) months.

Results The main changes in soil bacterial structure were observed at 8M and found to be modulated according to rock type, with petrochemistry and mineralogy acting as the main drivers. The content of microbial biomass carbon tended to decrease over time in the Control and KCl treatments, especially at 4M, while the rock treatments showed constant behavior. The sampling time and treatment affected the richness and diversity indices. The Si, Ca and Fe from mafic minerals were the main chemical elements related to the soil bacterial changes at 8M.

Conclusions The type (acidity) of silicate rock powder modulated the soil bacterial community (SBC) in a pot experiment with tropical soil. The specificity of the SBC for each rock type increased with time until the end of the experiment at 8 months (8M). The carbon content in the microbial biomass was lower in the rock powder treatments in the first month (1 M) than in the control and KCl treatments and was equal to or higher than that in the 8 M treatment. This result illustrates the challenge of modeling rock powder dissolution in soil since the soil medium is not inert but changes concurrently with the dissolution of the rock.

Keywords Geomicrobiology, Soil microbial activity, Crushed rocks, Agrominerals, Rock mineralogy

*Correspondence:
Antonio Carlos Azevedo
aazevedo@usp.br
Full list of author information is available at the end of the article

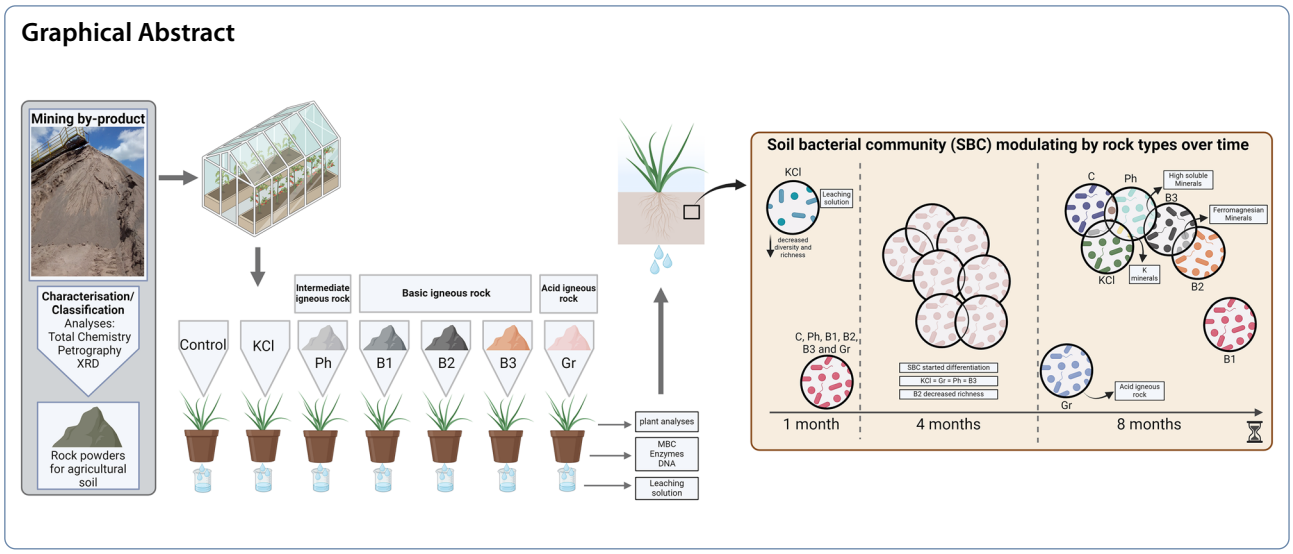

Background

Remineralization is an agricultural practice based on applying milled/crushed rock particles to the soil surface or at small depths to increase soil fertility and plant development [1]. The mechanisms by which plant growth improves when silicate rocks are applied to soil have not yet been completely elucidated. However, substantial data on the benefits of rock powder application in tropical agriculture have been obtained, especially for carbonate (limestone) and sulfate rocks (gypsum) [2, 3]. Despite the complexity of soil chemical dynamics in weathered soils under tropical or subtropical conditions, the agricultural use of silicate rock powders as soil amendments is strongly recommended. However, prior to its use, it is important to consider that the results are dependent upon several factors, such as the rock characteristics (e.g., chemical and mineralogical composition, particle size distribution), soil type, soil organisms, and plant species [4], because silicate anions tend to form less soluble solid phases than carbonate and sulfate anions.

Thus, it is reasonable that remineralization will take direct or indirect advantage of microbial activity, such as siderophore production, biofilm formation, enzyme activity, and various types of redox reactions [5–7]. Indeed, considering soil formation, biological activities (i.e., living organisms) accelerate the transfer of chemical elements from the lithosphere to the biosphere [8] and are one of the five factors involved in soil formation.

Rock powders are coproducts of several mining activities, such as aggregate production for construction and dimensional rocks. The powder generated by processing these rocks accumulates in the mining backyard in most cases, potentially causing problems in the management of the mining workflow and even environmental concerns, such as the source of air suspended and breathable particles [9].

The Brazilian territory is vast and is occupied by 63 M ha of cropland and 172 M ha of pastureland [10]; therefore, even the partial use of remineralizers as a soil amendment could have a substantial impact on saving natural resources and atmospheric carbon dioxide removal (CDR) [11]. Furthermore, the adsorption of contaminant effluent, a reduction in nitrogen emissions, and an increase in plant resistance to abiotic stress [4, 12] are concurrent benefits of rock powder use. However, it is important to think about the life cycle assessment of the use of rock powders beyond the agronomical benefits, considering the distance between the quarry and the place of application since these mining coproducts should not be transported too far [13].

The use of registered rock powder (remineralizer) has been regulated by Federal Laws in Brazil since 2013 [3]. Therefore, the correct use of rock powders as a soil amendment for agriculture has tremendous potential to boost the circular economy on a national scale. A major obstacle in the use of remineralizers is the lack of causal models to determine the outcomes of their use in agricultural and ecological scenarios [14, 15]. To help to fill this gap, it is paramount to identify how their use affects soil biological functioning, highlighting their impact on soil microbial community structure and soil microbiological attributes. To date, little is known about how bacterial community structures respond when different silicate rock powders are applied to soil, especially their response over time in short-term trials.

Therefore, in this investigation, the hypothesis that the soil bacterial community (SBC) structure responds differently to the type of silicate rocks applied to the soil in

short-term experiments based on the mineralogical and chemical composition of these rocks was tested.

Materials and methods

Experimental setup

The soil used in the experiment was classified as a Haplustox in Soil Taxonomy [16], a Haplic Ferralsol (loamic, aric) in the WRB [17], and a Latossolo Vermelho Amarelo Distrófico típico in the Brazilian Soil Classification System [18]. The 0–20 cm soil layer was collected at 21° 42′ 32.0″ S, 46° 51′ 42.0″ W in the state of São Paulo, Brazil, under a humid subtropical climate (Cwa) according to Köppen climate classification [19].

The soil and treatments were thoroughly mixed inside plastic bags before being dispensed into 3 L plastic pots. Five igneous rocks were chosen according to their Si content (acidic, intermediate and basic), mineralogy and petrochemistry and due to their K-bearing mineral content. The rocks were comminuted into a jaw crusher and then into a motorized mortar and pestle mill (Marconi, model MA890). Rock powders were prepared to have similar particle size distributions by combining 50% (m/m) very fine sand (VFS, from 0.10 mm to 0.05 mm), 25% medium sand (MS, from 0.5 mm to 0.25 mm) and 25% very coarse sand (VCS, from 2 to 1 mm). These fractions were chosen to maximize the ratio between the mass of the rock particles and the mass of the soil particles. Seven treatments were used: Control (C), KCl, phonolite (Ph), basalt 1 (B1), basalt 2 (B2), basalt 3 (B3), and granite (Gr). All basalts were collected from sites on the Serra Geral Formation in São Paulo State, where they are usually tholeiitic and contain small amounts of 2:1 phyllosilicate [20]. Phonolite and granite were collected from Minas Gerais State.

All treatments, except C and KCl, were amended with a single dose of 21 Mg ha^{-1} rock powder (considering the 0–20 cm layer and a soil density of 1.3 Mg m^{-3}) at the beginning of the experiment. KCl (0.3 Mg ha^{-1}; reagent grade, Merck) was applied as recommended by Novais et al. [21] for Brazilian soils as a function of the exchangeable K levels determined by soil fertility analysis. Treatment C followed the same procedure but without the addition of any amendments.

The experiment followed a randomized block design with 4 replicates, resulting in 28 experimental units (EUs). Because soil sampling was destructive, it was necessary to make three copies of the 28 EUs totaling 84 EUs so that one set of 28 EUs could be disassembled at each of the three time points reported here. We named each of these copies a replica, and they were spatially randomized among the other replicas. Therefore, one replica was disassembled after 1 month (1M replica), the second replica was disassembled after 4 months (4M), and the last replica was disassembled after 8 months (8M). After disassembling each replicate, aliquots of the soils were immediately stored at − 80 °C for further molecular analysis or at 4 °C for microbial biomass carbon and enzyme activity analyses.

The pots were sown with approximately 15 seeds of the tropical grass *Urochloa brizantha* (Hochst. Ex A. Rich.) STAPF. (syn. *Brachiaria brizantha* cv. Marandu), and after the first month, the most vigorous plant was selected, and the others were removed. The pots were maintained with 20% moisture on a dry mass basis [22]. Once a month, an extra 1 L of water was added, creating a leaching solution that was collected at the bottom of the pots. This procedure allowed us to evaluate the potential leaching of cations from the pots. When the plants reached approximately 40 cm in height, they were cut 15 cm above the soil surface to permit regrowth [23]. There was a total of 2 cuts during the 8 months of the experiment.

Chemistry and mineralogy of the soil and rocks

Soil chemical analyses were performed according to the standard methods for Sao Paulo State [24]. Briefly, soil-exchangeable bases (Ca, Mg, K) and P were extracted using the resin method. A 1 mol L^{-1} KCl solution was used to extract Al, while Ca phosphate and hot water were used to extract S and B, respectively. Cu, Fe, Mn and Zn were extracted using diethylenetriaminepentaacetic acid (DTPA). Na and Si were extracted using Mehlich 1 and 0.01 mol L^{-1} $CaCl_2$ (Additional file 1: Table S1).

Mineralogical analyses of the soil and the rocks were carried out in a Rigaku Miniflex II XRD benchtop system using CuKα radiation at 30 kV and 15 mA coupled to a graphite monochromator and a spinning sample holder. The samples were irradiated from 3 to 60° 2θ at 0.01° 2θ s^{-1}. X-ray diffraction (XRD) data were processed with "Match!" software (Cristal Impact, [25]), and minerals were identified using the COD reference database (Crystallographic Open Database) [26] and the mineralogical tables in Chen [27] and Brindley and Brown [28].

For total chemical analysis, soil and rock samples were air dried, homogenized and 10 g milled to a particle size of < 200 µm. Subsamples (0.25 g for rock, 0.1 g for soil) were subjected to two different analyses. One aliquot was fused with lithium metaborate ($LiBO_2$) in a muffle furnace and dissolved in an acid solution ($C_4H_6O_6$ and HNO_3). The elemental contents were determined by optical emission spectrometry (ICP–OS). Another aliquot was analyzed after multi-acid digestion (HCl, HNO_3, HF and $HClO_4$), and the elemental content was determined by inductively coupled plasma–mass spectrometry (ICP–MS). This analysis was performed to quantify the total elements in each rock powder, linking them to the

minerals identified in the mineralogical analysis (XRD) and the dissolved elements in the pot leachate.

Petrographic slides were made by selecting a particular area on each rock sample. Each sample was impregnated with industrial Araldite, and the resulting block was sawed and glued to a glass slide and then brought to a thickness of 0.03 mm (30 μm). The slides were observed under a Nikon Eclipse 50iPol petrographic microscope with transmitted light and plane-polarized with image capture to be described. This analysis was performed to characterize the rocks in terms of the types of minerals present (to support the XRD data) and to observe the shape and size of the rock minerals, which also differed among the three basalts tested.

Microbial biomass carbon (MBC) and enzyme activities

MBC was extracted from the soil using the fumigation-extraction method and the content was determined by titration according to Vance et al. [29]. Briefly, 10 g of soil was adjusted to have 40% of its maximum water holding capacity and then placed in an evacuated desiccator. For each soil sample, both ethanol-free chloroform-fumigated and nonfumigated samples were left in the dark for 24 h. Then, the soils were extracted with 0.5M K_2SO_4 solution (4:1, v/w) to determine the carbon content by titration with 0.033M $(NH_4)_2Fe(SO_4)_2$ $(H_2O)_6$ (Mohr's salt).

Acid phosphatase (EC 3.1.3.2), β-glucosidase (EC 3.2.1.21), and arylsulfatase (EC 3.1.6.1) activities were evaluated due to their direct roles in phosphorus, carbon, and sulfur cycling in the soil, respectively, and were determined following the methodology proposed by Tabatabai [30]. Briefly, for acid phosphatase, 1 g of soil was incubated with modified universal buffer (MUB) at pH 6.5 along with the *p*-nitrophenyl-phosphate (PNF) substrate at 37 °C for 1 h, and extraction solution composed of 0.5M $CaCl_2$ and 0.5M NaOH was added. β-Glucosidase assays were performed with MUB at pH 6 with *p*-nitrophenyl-β-D-glucoside (PNG) as the substrate, and arylsulfatase assays were performed with 0.5M sodium acetate buffer at pH 5.8 with *p*-nitrophenyl sulfate (PNS) as the substrate. In each case, the samples were incubated, the extraction solutions were added, the samples were filtered through a No. 2 Whatman filter, and the color intensities were measured at 410 nm using a spectrophotometer (EZ Read 400, Biochrom). Enzyme activities were determined based on a standard curve developed with a ρ-nitrophenol solution.

DNA extraction and SBC structure assessment

Total DNA was extracted from 0.4 g of each of the 84 soil samples using a commercial kit (PowerSoil DNA Isolation, MoBio, Carlsbad, CA, USA) following the manufacturer's instructions. The integrity of the DNA was verified using gel electrophoresis (1% agarose) prior to performing PCR assays, and the quantity of DNA was measured using a Qubit fluorimeter (Invitrogen, Carlsbad, CA).

The bacterial community structure was determined by terminal restriction fragment length polymorphism (T-RFLP) of the bacterial 16S rRNA gene using soil DNA amplified with the primers 8-FM (5′-6AGAGTT TGATCMTGGCTCAG-3′) and 926r (5′-CCGTCA ATTCCTTTRAGTTT-3′) [31] in triplicate. The primer 8-FM was labeled with 6-carboxyfluorescein (6-FAM). The reaction mixture consisted of 1 μl of DNA template (approximately 50 ng), 4 μl of dNTPs (0.2 mM), 0.1 μl of each primer, 5 μl of PCR Buffer X10, 6 μl of $MgCl_2$ (50 mM) and 0.2 μl (1 U) of platinum Taq DNA polymerase (Sinapse Inc., São Paulo) in a final volume of 50 μl. Amplification was carried out with the following cycling conditions: 95 °C for 4 min, followed by 30 cycles of 95 °C for 30 s, 53 °C for 30 s and 75 °C for 45 s and a final step at 72 °C for 10 min, with a procedure modified from those of Durrer et al. [32] and Pimentel et al. [33].

Aliquots of PCR amplicons (approximately 200 ng) were digested with the restriction enzyme Hhal (10 U/μl) (Thermo Scientific) at 37 °C for 3 h. The digested material was then precipitated with 2 μl of 3M Na-acetate, 2 μl of 125 mM EDTA and 50 μl of absolute ethanol and centrifuged at 4000 rpm for 30 min. The precipitated DNA was washed with 70% ethanol and dried by centrifugation. The DNA was suspended in formamide Hi-DiTM (Applied Biosciences, Foster City, CA) and analyzed on an ABI Prism 3500 automatic sequencer (Applied Biosystems, Life Technologies). A threshold of 50 units of fluorescence was adopted to remove the background of the samples, and the results were transformed into a relative abundance matrix of the peak areas.

The T-RFLP technique provided us with a matrix based on the number and peak heights or areas of the terminal restriction fragments (TRFs), which were separated with an automated DNA analyzer [34]. As with all techniques in molecular biology, when using the fingerprinting technique, there are several bottlenecks regarding full-scale application for some ecological approaches, such as the evaluation of functions and species composition [35]. However, the use of T-RFLP is not obsolete and is still highly valuable for studying microbial community dynamics [36–39]. Over the past decade, high-throughput sequencing has transformed soil ecology studies by enhancing our ability to discern taxonomic identities, particularly when designated sequence data are accessible. However, as demonstrated by Lindström et al. [40], both T-RFLP and high-throughput sequencing methodologies effectively capture similar spatiotemporal

variations, providing comparable insights into the functional and taxonomical details of the microbial communities in the soil.

Leachate and plant tissue analyses

Leaching solutions were collected, and the volume, pH, electrical conductivity (EC) and temperature were immediately measured. Then, the pH of each leachate was adjusted to 3 with 3% nitric acid (added dropwise) to prevent precipitation and microbial growth, and the leachate was stored in 15 mL plastic tubes at 5 °C until ICP–OES analysis [41]. The aboveground plant tissue was collected and dried at 60 °C, the biomass weight was measured on a dry basis, and aliquots (0.25 g) were put into Teflon vessels and subjected to microwave acid digestion in a Mars Xpress (CEM) with 2 mL of hydrogen peroxide and 4 mL of nitric acid. The heating gradient was as follows: to 80 °C over 3 min, 150 °C over 10 min, 180 °C over 10 min and finally 180 °C over 5 min. The extract volume was adjusted to 35 mL with ultrapure water before analysis by ICP–OES [42] to quantify the absorbed elements (this paper presents the K content only).

Data analyses

One-way ANOVA was used to evaluate the K, Ca and Na concentrations in the leachate and plant tissue to verify their significance after the assumptions for ANOVA (homogeneity and normality) were met. Wald tests were used for the soil microbiological attributes (microbial biomass carbon and enzyme activities) in R software (version 3.6.3) (R Core Team 2016).

Changes in the SBC structure were evaluated based on the Bray–Curtis distances of the relative abundance of the peak area matrix obtained from the T-RFLP. The Shannon–Weaver and richness indices of the TRFs were calculated according to Zhang et al. [43].

Although ecological diversity indices are frequently applied to fingerprinting methods, multiple taxa can generate the same TRF, and rare TRFs can be excluded by a relative abundance threshold [44]. To determine the differences in the SBC structures between different treatments amended with silicate rocks, we performed nonmetric multidimensional scaling (NMDS) coupled with PERMANOVA (ANOSIM function in R, permutations = 999) considering the relative abundance of the peak area matrix transformed into log (x + 1) [45]. We carried out global redundancy analysis (RDA) coupled with a forward selection function to verify the most representative mineralogical properties (see Additional file 2: Table S2). Diversity, richness, and PERMANOVA were performed using the vegan package in R software [46].

A structural equation model (SEM) was adopted to explore how the most representative mineralogical rock attributes obtained from the NMDS ($r^2 > 0.75$; Table 2D) influenced the SBC structure at the most impacted sampling time (8M). For this purpose, the C and KCl treatments were not considered because they were not amended with silicate rocks. First, we used NMDS to determine the first axis scores, which were used as indicators of bacterial community structure (composite variable) [47–49]. We used a minimum set of parameters to assess the model fit, including the comparative fit index (CFI), root mean square error of approximation (RMSEA), and Tucker–Lewis index (TLI), using the benchmark values according to Fan et al. (2016). The modeling process was performed using the lavaan [50] and semPlot [51] packages. In our SEM, we plotted the *std.all*, which determines the standardized coefficient for the path. As a result, coefficients above 1 can be observed. On the other hand, when employing the *std.lv*, which standardizes to the latent factors, coefficients typically range from −1 to 1. The original data and scripts used are provided in the Additional file.

Results

Mineralogy of the soil and rocks

XRD of the sand fraction of the soil showed only quartz, and no easily bioweatherable primary minerals were identified. Kaolinite and gibbsite were the major minerals in the clay fraction. Therefore, the degree of desilication of the soil was between that of monosialitization and that of allitization (Fig. 1A).

We assign, based on the XRD, total chemical and petrography analyses, that the phonolite had mica (Mca), alkali feldspar (sanidine—Sa), feldspathoid (nepheline—Nph), sodium pyroxene (Aeg—aegirine), eudialyte (Eud) and zeolite (natrolite—Ntr), which are K- and Na-rich minerals (Fig. 1C), which contributed to the high contents of K_2O and Na_2O in the chemical composition of this rock (Table 1). Mineralogy of the basalts was similar, with dominant plagioclase (Pl) and pyroxene (Px-augite) (Fig. 1C). However, B1 has more magnetite (Mag) and pyroxene (Px), while B2 and B3 have more olivine (Ol) and zeolite (Hul—heulandite), respectively. The structures and textures of the basalts are diverse. B1 is microcrystalline, while B2 has a coarser texture, and B3 has cavities and amygdales filled with zeolite (Hul—heulandite) (Fig. 2D). Zeolites are very reactive silicates that have a large surface area and cation exchange capacity (CEC). The variations in chemistry (Table 1), mineralogy (Fig. 1B) and structure (Fig. 2) of these basalts were used to test the sensitivity of the SBC structure to small variations in the characteristics in a single rock group. Gr was the only acid rock used (SiO_2 greater than 52%, i.e.,

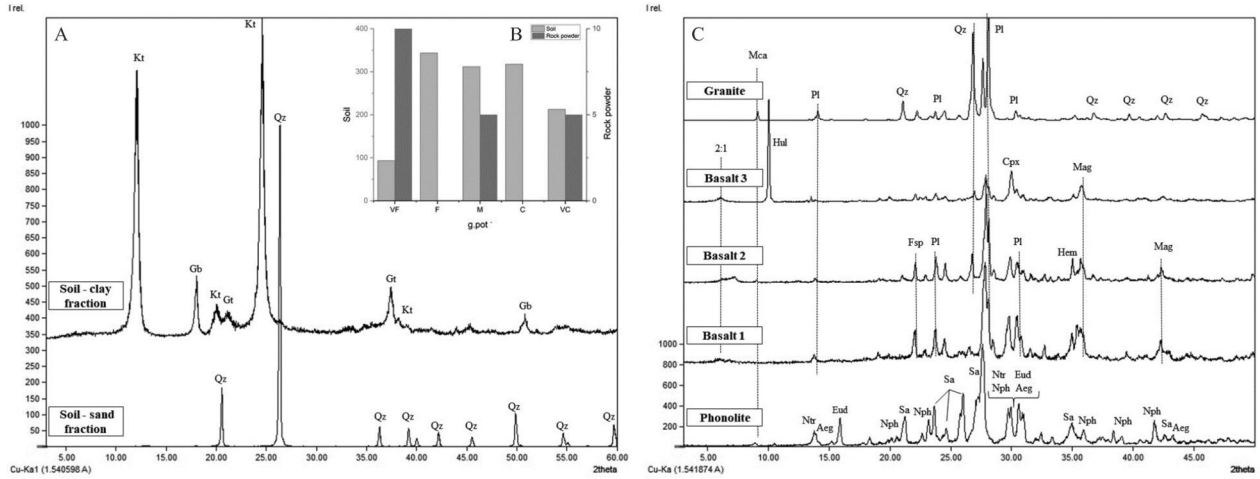

Fig. 1 X-ray diffractometry depicting the mineralogy of the (**A**) soil (Gb: gibbsite; Gt: goethite; Kt: kaolinite; and Qz: quartz) and rocks (**C**) used in the experiments (Aeg: aegirine; Cpx: clinopyroxene; Eud: eudialite; Fsp: feldspar; Hem: hematite; Hul: heulandite; Mag: magnetite; Mca: mica; Ntr: natrolite; Nph: nepheline; Pl: plagioclase; Qz: quartz; and Sa: sanidine). **B** Textures of the soil and rock powders (VF: very fine, F: fine, M: medium, C: coarse, and VC: very coarse)

Table 1 Total chemical compositions of the initial soil and rock samples determined via ICP–OS

Element	SiO_2 %	Al_2O_3 %	Fe_2O_3 %	CaO %	MgO %	Na_2O %	K_2O %	MnO %	P_2O_5 %	LOI* %
Soil	69.36	14.10	5.14	0.34	0.09	0.03	0.33	0.05	0.09	8.47
Phonolite	56.4	20.9	3.87	1.76	0.32	6.74	8.05	0.25	0.07	2.83
Basalt 1	50.6	12.15	15.1	7.59	3.82	2.66	1.5	0.21	0.61	1.45
Basalt 2	47.7	11.8	16.1	9.03	5.77	2.41	1.09	0.22	0.45	1.61
Basalt 3	48.8	11.9	13.25	8.99	4.64	2.43	1.15	0.19	0.21	5.44
Granite	76.7	13.8	1.14	0.43	< 0.01	4.68	3.87	0.16	< 0.01	0.51

*Loss on ignition

Si greater than 24.3%) [52] (Table 1), which explains the abundant quartz (Qz) peak in the XRD pattern and the abundances of plagioclase (Pl) and mica (Mca) (Fig. 1B).

Soil microbiological attributes

The MBC in treatments C and KCl decreased over the evaluation time ($p < 0.05$), while for treatments with rock powders, with the exception of Gr, there was a decrease from 1 to 4 M, followed by an increase to 8M, restoring the levels to the same values as those in the first evaluation (1M) (Fig. 3A). At 1M, the MBC in the C and KCl treatments was greater than that in the other treatments, and the MBC in the Ph treatment was intermediate between that in the C and KCl treatments and that in the other silicate rocks. At 4M, the MBC was highest in the KCl treatment group and lower in the other groups. However, at 8M, the opposite trend was observed, and KCl had the lowest MBC while B2 had the highest MBC (Fig. 3A).

The enzyme activities varied according to treatment and evaluation time, but a clear pattern among them was not identified.

The activity of β-glucosidase decreased in treatments C and B1 ($p < 0.05$) over the evaluated periods. The activity of this enzyme at 1M outperformed that in the other times in treatment C, as opposed to that in the Gr treatment. The activity of β-glucosidase in the Gr treatment group increased at 4M but decreased again at 8M ($p < 0.05$) (Fig. 3B). There was no significant difference among the treatments at 4M. However, at 8M, the KCl and Gr treatments presented the highest and lowest activity, respectively ($p < 0.05$) (Fig. 3B).

The arylsulfatase activity at 1M was the greatest for treatments B3 and Gr, followed by B2, B1 and Ph, and significantly lower activity was observed for treatments C and KCl (Fig. 3C). The treatments did not differ at 4M. At 8M, Ph had the highest activity of arylsulfatase, and B3 had the lowest. Over time, the arylsulfatase activity continuously decreased in treatments B2, B3 and Gr until the

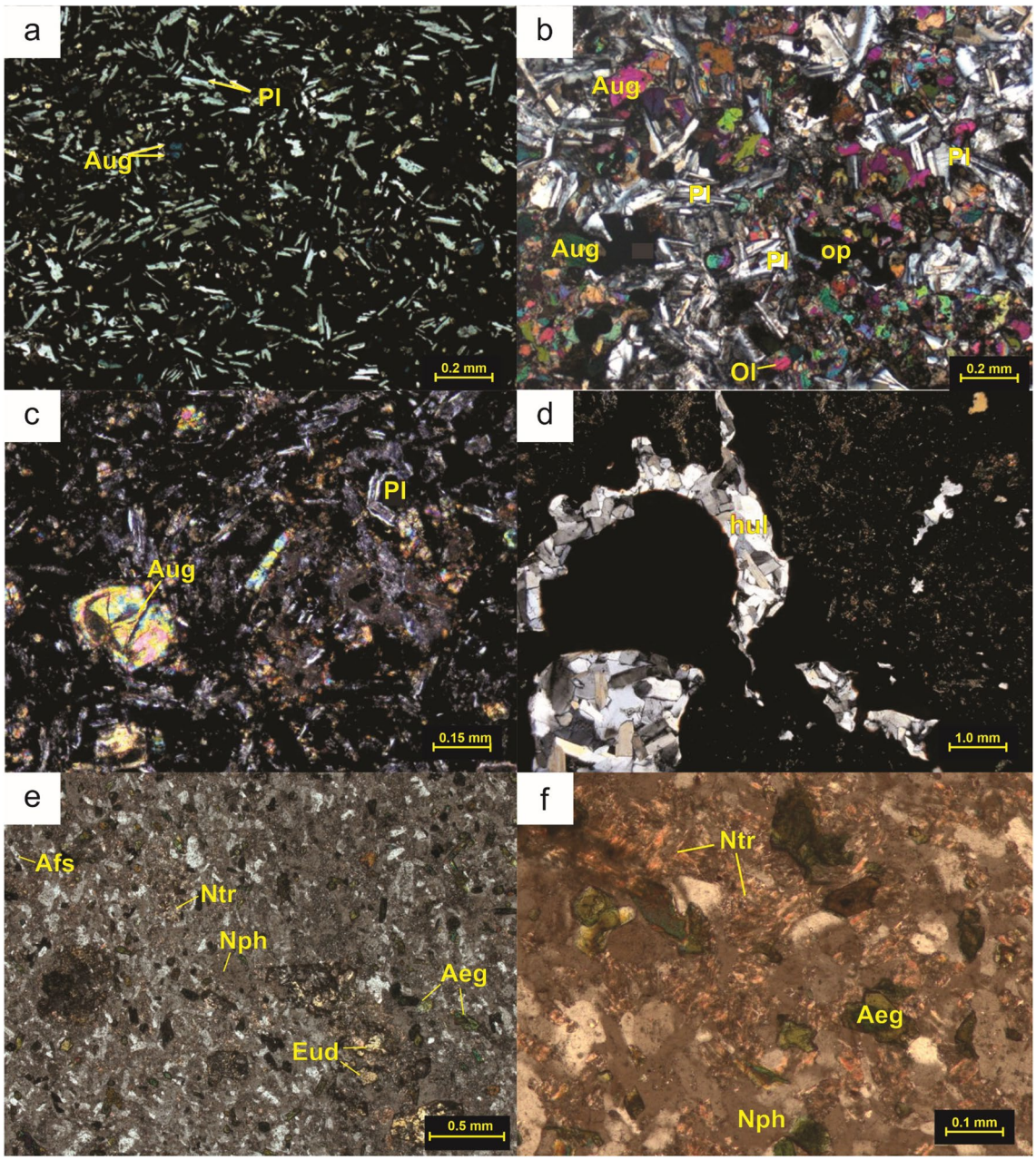

Fig. 2 Petrographic characterization of basalts and phonolite. **A** basalt 1, **B** basalt 2, **C** basalt 3, **D** heulandite (Hul)—basalt 3, **E** phonolite and **F** natrolite (Ntr)—phonolite

end of the experiment at 8M, while that in treatment C increased at 4M.

The acid phosphatase activity in the KCl treatment group was the highest among all groups at 1M and the lowest in C and B3 at this time ($p < 0.05$) (Fig. 3D). At 4 M, there was a general increase in acid phosphatase activity in C, Ph, B1 and B3 (see small capital letters in Fig. 3D) compared to those at 1M. In particular, C had the greatest increase in acid phosphatase activity, while B2 had the lowest when comparing all the treatments at 4M. At 8M, the KCl treatment showed the highest acid phosphatase activity, and B1 had the lowest activity. The activity of this enzyme in the basalts consistently lower during the experiment. Despite its presence in a small amount (maximum of 0.61% P_2O_5, Table 1), this seemed to be sufficient to impact the phosphorus metabolism of the bacteria. In addition, we observed

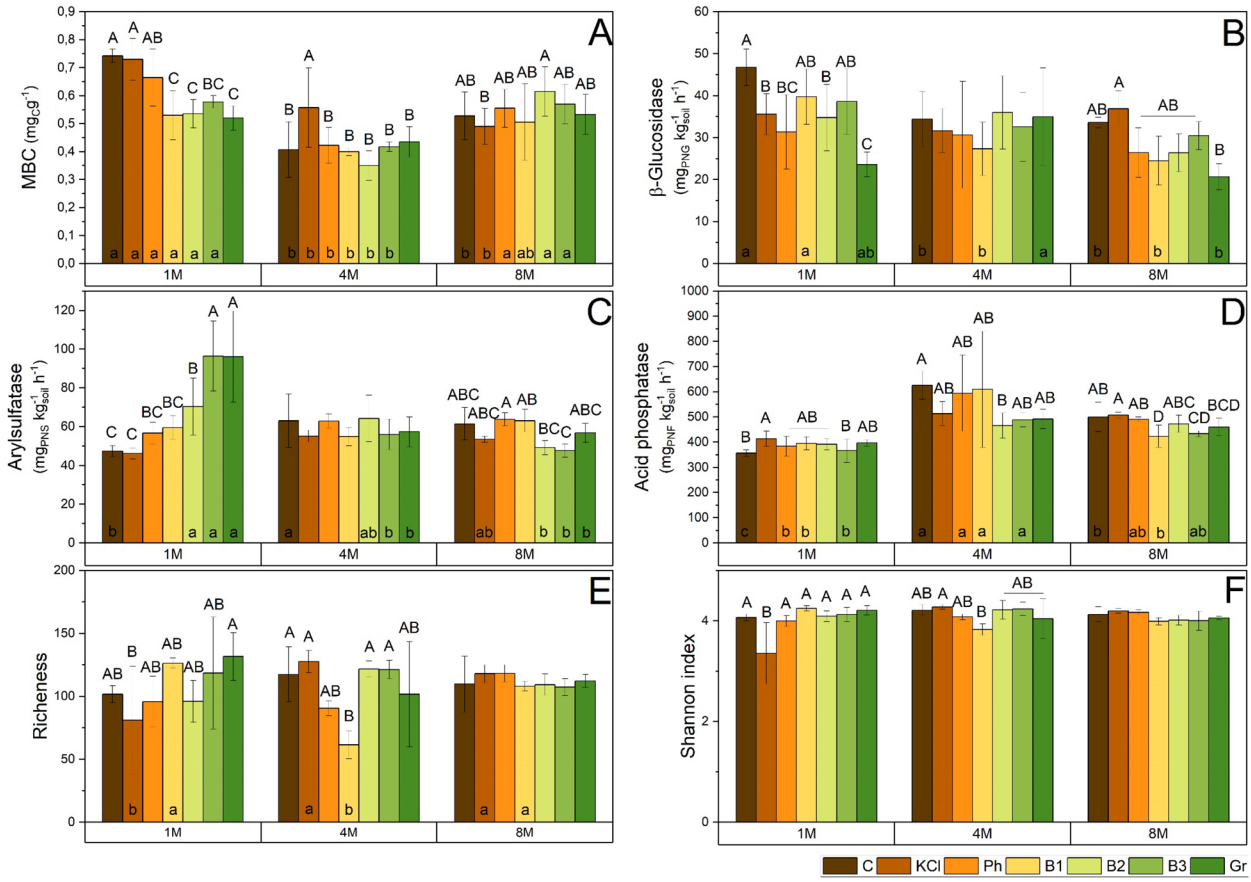

Fig. 3 Response of soil microbiological attributes. **A** Microbial biomass carbon (MBC), **B** β-glucosidase activity, **C** arylsulfatase activity, **D** acid phosphatase activity, **E** richness and diversity and **F** Shannon index under the different treatments (C: control; KCl; Ph: phonolite; B1: basalt 1; B2: basalt 2; B3: basalt 3; and Gr: granite) over time: after 1 month (1M), 4 months (4M) and 8 months (8M). Lowercase letters indicate the same treatment over time. Capital letters indicate that the different treatments were compared at the same time by the Wald test ($p < 0.05$). The absence of any letters indicates that there was no significant difference

that treatments C, Ph, B1 and B3 had increased acid phosphatase activity at 4M.

The richness index of the bacterial community fluctuated ($p < 0.05$) over time for the KCl and B1 treatments only (see the small capital letter results in Fig. 3E). At 1M, KCl showed the lowest richness and Shannon indices, which increased at the following evaluation times (4M and 8M) along with the exhaustion of this source. In B1, there was a drastic decrease in these indices at 4M, which recovered at 8M. At each time point, the lowest richness index was observed in KCl, while the highest was observed in Gr at 1M. At 4M, the lowest richness index was observed in B1, whereas at 8M, there were no differences between the treatments and the control (Fig. 3E).

In terms of the Shannon index, at 1M, the only difference was the lowest value in the KCl treatment group ($p < 0.05$), while at 4M, the value in the KCl group was the highest, and that in the B1 group was the lowest. Finally, at 8M, there were no differences among the treatments (Fig. 3F). The Shannon index was the only microbial index evaluated that did not vary throughout the experiment (lack of small capital letters in Fig. 3F).

NMDS analysis revealed that the bacterial community structure changed over time. The greatest variation was observed with KCl treatment at 1M (Fig. 4A), which lacked an adjustment along with the other treatments at 1M. Thus, the KCl treatment results are shown in Fig. 4B, and there was no significant difference among the other treatments (Table 2).

After four months (4M) (Fig. 4C), the initially strong effect of KCl diminished, but the conditions did not completely return to those of treatment C. However, KCl treatment also did not differ significantly from Ph, B3 or Gr. On the other hand, the effects of some of the rock powders started to appear, since the Ph, B1 and B3 treatments clustered ($p < 0.05$) (Table 2).

At 8M, three clusters were identified: one formed by C, KCl and Ph in the left quadrant; one with all the basalt

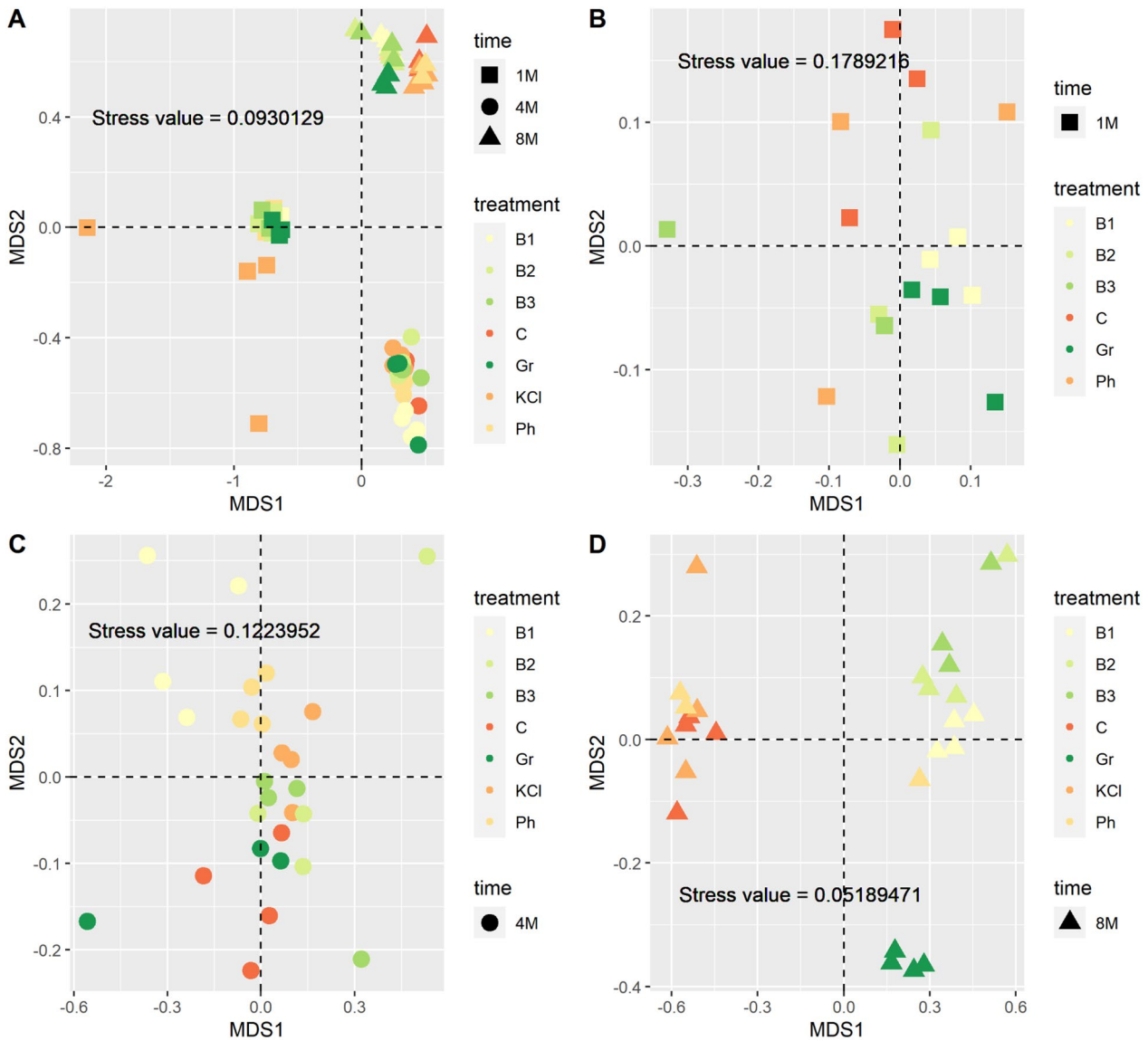

Fig. 4 Nonmetric multidimensional scaling (NMDS) of the bacterial community structure in the three periods (**A**) and after 1 month (1 M) (**B**), 4 months (4M) (**C**) and 8 months (8M) of the experiment (**D**)

rock powder treatments in the upper right quadrant; and Gr treatment (Fig. 4D). ANOSIM confirmed the similarity of the bacterial community structure among basalt-treated soils B2 and B3; however, B1 differed ($p < 0.05$). Moreover, no significant difference was found between Ph and B3 (Table 2).

The SEM indices of goodness of fit ($X^2 = 19.007$, p-value = 0.001, CFI = 1.00, TLI = 1.00, RMSEA = 0.00) were acceptable, with an R^2 value of 0.65. Overall, the mineralogical attributes positively affected the SBC structure. From the total chemical analysis, Si, Ca, and Fe showed the highest standardized path coefficients for bacterial community structure (1.29, 1.00, and 0.94, respectively), but only Si was significant ($p < 0.05$). Moreover, only Mg was negatively associated with the bacterial community structure (−0.20) (Fig. 5).

Elements in the leachate and plant tissue

Only KCl significantly differed ($p < 0.001$) from the other treatments in terms of K leached (mg), and the K content in the plant tissue was similar among all the treatments (Table 3). At 8M, the total amount of K leached from the pots after KCl treatment was approximately 30 times greater than the amount leached from Ph treatment,

Table 2 Analysis of similarity (ANOSIM) of the bacterial community structure amended with distinct rock powders **A** throughout the experimental period and at the following time points: **B** 1 month (1M), **C** 4 months (4M), and **D** 8 months (8M). **E** Global multidimensional scaling (NMDS) output showing the r^2 and significance values that explain the strength of the association between all of the rock chemical elements and nonmetric multidimensional scaling (NMDS1 and NMDS2)

(A)						***p*-value**
Time						**1M**	**4M**
1M						-	–
4M						0.001***	-
8M						0.001***	0.001***
(B)	***p*-value—1 month (1M)**						
Treatment	T1-C	T3-Ph	T4-B1	T5-B2	T6-B3		
Control	–	–	–	–	–		
Phonolite	0.80	–	–	–	–		
Basalt 1	0.10	0.09	–	–	–		
Basalt 2	0.20	0.30	0.60	–	–		
Basalt 3	0.23	0.23	0.31	0.31	–		
Granite	0.10	0.10	0.40	0.30	0.35		
(C)	***p*-value—4 months (4M)**						
Treatment	T1-C	T2-KCl	T3-Ph	T4-B1	T5-B2	T6-B3	
Control	–	–	–	–	–	–	
KCl	0.03*	–	–	–	–	–	
Phonolite	0.03*	0.06	–	–	–	–	
Basalt 1	0.03*	0.03*	0.05	–	–	–	
Basalt 2	0.06	0.03*	0.03*	0.03*	–	–	
Basalt 3	0.09	0.55	0.08	0.03*	0.57	–	
Granite	0.43	0.14	0.03*	0.06	0.17	0.45	
(D)	***p*-value—8 months (8M)**						
Treatment	T1-C	T2-KCl	T3-Ph	T4-B1	T5-B2	T6-B3	
Control	–	–	–	–	–	–	
KCl	0.42	–	–	–	–	–	
Phonolite	0.51	0.62	–	–	–	–	
Basalt 1	0.03*	0.03*	0.03*	-	–	–	
Basalt 2	0.03*	0.03*	0.03*	0.03*	–	–	
Basalt 3	0.03*	0.03*	0.10	0.03*	0.97	–	
Granite	0.03*	0.03*	0.03*	0.03*	0.03*	0.03*	
Rock chemical element						r^2	***p*-value**
Si						**0.840**	**0.001 *** **
Al						0.625	0.003 **
Fe						**0.787**	**0.001 *** **
Ca						**0.843**	**0.001 *** **
Mg						**0.792**	**0.001 *** **
Na						0.714	0.001 ***
K						0.708	0.001 ***
Mn						0.647	0.002 **
P						0.463	0.005 **

* (0.05); ** (0.01); *** (0.001)

The most representative ($r^2 > 0.75$) attributes used in the structural equation model (SEM) are shown in bold

SEM model = bacteria structure ~ Si + Fe + Ca + Mg

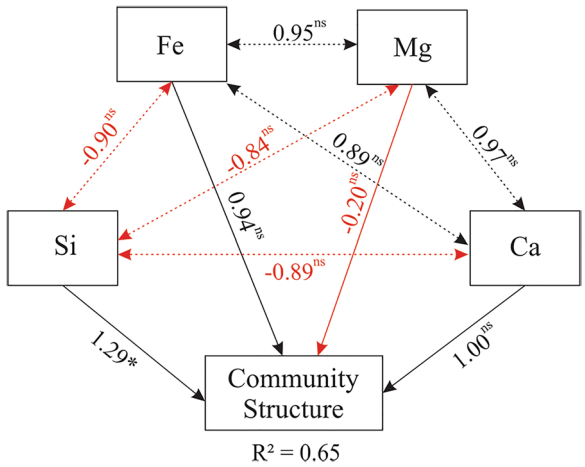

Fig. 5 Structural equation model (SEM) representing the complex interrelationships between the most representative ($r^2 > 0.75$) mineralogical rock traits according to NMDS analysis and their influence on the soil bacterial community structure at 8M. Values associated with solid or dashed arrows represent significant standardized path coefficients with direct and indirect correlations, respectively. Red arrows indicate negative correlations, while black arrows indicate positive correlations. The R^2 values associated with the bacterial structure indicate the proportion of variation explained by correlations with other variables. ns: not significant, $^*p < 0.05$

which is the rock with the greatest concentration of K (Table 3). In addition, the greater K concentration in the KCl solution induced greater Ca leaching, mainly at 1M.

Discussion

In this paper, we tested the sensitivity of the SBC and soil bioindicators to the presence of igneous rock powders (basic, intermediate, and acidic) during an 8-month experimental period.

After one month (1M), KCl was the only treatment that caused a change in the SBC structure, as indicated by NMDS analysis (Fig. 4A). Such a drastic change in SBC structure is known to occur as a result of the use of highly soluble fertilizers [53–56]. This change was also observed in the richness and Shannon indices, which were the lowest at 1M in the KCl group (Fig. 3E and F), revealing its impact on the SBC. A similar reduction in richness was observed by Ben Zineb et al. [57] for a treatment with super triple phosphate as opposed to the increase in richness with phosphate rock treatment according to the plant and dose used. This contrasted with the application of silicate rock powders.

In the experiment presented here, this change was possibly caused by the large amount of K and Cl ions solubilized in the system. The concentration of K from a single leaching event at 1M ranged from 0.0 mg L^{-1} to 31.79 mg L^{-1} in all but the KCl treatment, which ranged from 12.34 mg L^{-1} to 1022.00 mg L^{-1} (data not shown). Therefore, despite K being a macronutrient [58], the K concentration in KCl reached more than 15 times the optimal concentration for bacterial growth, which is approximately 60 mg L^{-1} [59].

K and Cl ions have similar hydration enthalpies ($K^+ = -321$ J K^{-1} mol^{-1}; $Cl^- = -363$ J K^{-1} mol^{-1} [60]), which leads to the formation of large hydration shells and a more negative soil water potential, decreasing water flow into the cell [61]. Microbial cells alter their metabolism to compensate for fluctuations in the osmotic potential of the surrounding solution [62]. Therefore, the great change in the SBC in KCl seemed to be triggered by changes in the nutrient and water status of the surrounding environment of the bacteria.

The extremely high concentration of K^+ in the soil solution in KCl at 1M also induced an increase in the loss of Ca^{2+} via the leachate (Table 3). Variations in the availability of Ca also impact the SBC [63].

The large amounts of Na in the Ph (6.74% Na_2O and 4.76% Na, Table 1) and Gr (4.68% Na_2O and 3.4% Na, Table 1) rocks were not released fast enough to increase the Na concentration in solution and significantly change the SBC structure (Table 3). Similar to K ions, Na ions have a large hydration shell and very negative hydration enthalpy (-405 J K^{-1} mol^{-1}).

The covalent character of the Si–O bond implies that silicate rock powders will have a lower solubility and greater buffering capacity than the K–Cl bond with ionic character, which results in greater solubility [64–66]. This can be shown by comparing the release of K from KCl and Ph. The chemical composition of KCl was 41.5% K (60% K_2O, m/m), while that of phonolite was 5.45% K (8.0% K_2O, m/m). The KCl/Ph K content ratio was 7.6 in the solid phase, while in the leaching solution, this ratio was 41.88 at 1M (Table 3).

The high solubility of KCl led to its quick exhaustion, causing the SBC to cluster to the Ph, B3 and Gr groups at 4M ($p < 0.05$) (Fig. 4C, Table 2), which is interesting because these rocks have higher K concentrations (Ph and Gr) and higher reactivity (Ph and B3) than the other rocks. As leaching continued from 1 to 8M, KCl tended to cluster with the other treatments (Fig. 4D, Table 2). However, at 4M and 8M, while the SBC in the pots treated with rock powders moved farther from C, KCl reverted. This was also observed by Cuhel et al. [67] in a long-term field trial. At the end of our experiment (8M), the richness and Shannon indices did not differ between treatments (Fig. 3E and F), which is in contrast to the results of Mickan et al. [68], in which the effects of soluble fertilizer and rock powder (75 kg ha^{-1} mix rocks and minerals with ammonia sulfate and potassium sulfate) reduced the microbial diversity after 10 months.

Table 3 Cumulative K, Ca and Na leached from the 1M, 4M and 8M replicas, total K in aboveground plant tissue, and plant dry biomass

Treatment	K leachate (mg)				K plant (mg)	Ca leachate (mg)				Na leachate (mg)				Dry biomass (mg)
	1M	4M	8M	total		1M	4M	8M	Total	1M	4M	8M	Total	
Control	20.80 b	7.46 b	8.70 b	36.96 b	96.89 a	30.65 b	11.43 b	27.60 b	69.67 b	30.65 b	11.43 b	27.60 ab	69.67 b	5996.7 a
KCl	774.45 a	245.71 a	85.44 a	1105.59 a	101.79 a	209.17 a	29.12 a	17.93 bc	256.22 a	209.17 a	29.12 a	17.93 b	256.22 a	4790.0 a
Phonolite	18.49 b	10.43 b	7.27 b	36.19 b	94.13 a	30.65 b	10.15 b	21.50 b	62.30 b	30.65 b	10.15 b	21.50 ab	62.30 b	6243.3 a
Basalt 1	20.96 b	5.40 b	8.55 b	34.92 b	71.19 a	37.03 b	9.01 b	24.91 b	70.95 b	37.03 b	9.01 b	24.91 ab	70.95 b	4020.0 a
Basalt 2	17.49 b	7.23 b	8.62 b	33.34 b	70.54 a	31.79 b	9.19 b	21.25 b	62.22 b	31.79 b	9.19 b	21.25 ab	62.22 b	3960.0 a
Basalt 3	17.36 b	5.12 b	9.87 b	32.34 bc	78.25 a	37.66 b	10.88 b	31.52 ab	80.06 b	37.66 b	10.88 b	31.52 a	80.06 b	4720.0 a
Granite	14.79 b	6.98 b	7.18 b	28.96 c	92.57 a	26.81 b	10.72 b	27.62 b	65.15 b	26.81 b	10.72 b	27.62 ab	65.15 b	5530.0 a

The different letters indicate significant differences according to Tukey's test ($p < 0.05$)

However, we need to consider the differences in the dose and composition of the rock powder between the present work and that of Mickan et al. [68].

Concurrently, the amounts of K^+ and Ca^{2+} in the leachate of KCl also decreased due to exhaustion (Table 3), demonstrating the strong influence of soil solution characteristics (such as ionic activity and osmotic potential) on SBC dynamics.

The SBC discriminated the major rock types at 8M: the basalts (B1, B2 and B3) clustered in the right upper quadrant of the NMDS (Fig. 4D) and Ph, C and KCl clustered in the left quadrant, while the Gr was in the lower quadrant. In fact, the SEM confirmed that the Si content in the rocks significantly positively affected the bacterial community (Fig. 5), although Fe and Ca were also positively correlated.

Beyond the Si content, the SBC was also sensitive to small variations in rock characteristics (texture, mineralogy and chemistry—Table 1, Fig. 1C and Fig. 2A–C), as inferred from the dissimilarities of the SBCs among the basalt varieties (significant difference at $p < 0.05$ among B1 at 8M but no significant difference between B2 and B3, Table 2).

The amounts of Si in Ph and in the basalts (B1, B2 and B3) were similar (Table 1). However, these rocks are classified differently because of the conditions under which they crystallize, their chemical composition, and, therefore, the minerals they form. The nepheline in Ph is a feldspathoid mineral that releases Ca, Na, and K faster than the plagioclase (Ca-Na feldspar) present in the basalts. The SBC seemed to be sensitive to such differences since Ph differed from Gr and all the basalts except B3 (Table 2) at the end of the experiment (8 M). This similarity in the SBC between Ph and B3 (Table 2) may be related to the common presence of a small amount of zeolite (heulandite in B3 and natrolite in phonolite; Fig. 2D and F). Zeolite minerals are rich in Ca and Na and have great surface reactivity and porosity. These relationships highlight the importance of understanding not only the total chemistry but also the mineralogy of the rocks since the presence of highly reactive minerals, even in small amounts, may surpass the effects of the less reactive minerals in the rock, even in greater amounts, at least during the initial stages of dissolution.

The SBC structure in the Gr treatment group was similar to that in the basalt group at the beginning of the experiment (1M), as shown by NMDS analysis, but ended the experimental period (8M) (Fig. 4D) distinctly ($p < 0.05$) (Table 2). In fact, previous works also revealed changes in the soil microbiome composition caused by the presence of rock powder, but they did not compare different rock powders or durations [57, 69].

However, we observed clear responses regarding the structure of the bacterial community, whether due to the rapid effect of KCl after 1M or its slow evolution caused by the rock powders, and the effects of these treatments on soil bioindicators were unclear. Several studies have used soil bioindicators to evaluate soil management [70–74] and textural classes [75] in tropical soils. However, studies evaluating the effects of rock powders are scarce, and even so, comparisons are difficult due to the different sources and doses of rocks, soil, plants, enzymes and durations evaluated. In the present study, an exception was the consistent low activity of acid phosphatase in the basalt treatments (B1, B2, and B3). These rocks had between 2 and approximately sixty times more P_2O_5 (as apatite) in their composition than the other rocks. This enzyme activity was particularly low at 8M (compared to the other treatments at the same time), which may be related to the greater dissolution of apatite at the end of the experiment due both to its low solubility and to the increase in grain porosity and apatite accessibility as the experiment progressed. The greater availability of P seemed to result in lower acid phosphatase activity, which corroborates the literature [76].

The present results showed that, although crop performance was not affected by rock powders in the short term (see K in plant and biomass production in Table 3), the SBC was. Regarding the rock powder treatments, the SBC started showing significant alterations only at 8M. The rock powders did not cause extreme or rapid changes in the bacterial diversity of the soil (Fig. 4A and B) and possibly caused less disruption to the microbial-plant cooperative processes active in the rhizospheric environment, such as nutrient absorption and pathogen protection [77]. In fact, Cui et al. [53] observed that the use of NPK decreased SBC richness and increased the abundance of specific groups, decreasing the redundancy and, consequently, the resilience of the SBC. This is related to the large and rapid changes in the soil chemical environment caused by high doses of KCl, as observed in the present study.

This paper contributes to a better understanding of the interplay among rock powders and their impact on the structure of the SBC and bioindicators in the soil. As stated by Swoboda et al. [4] in their review, the duration of a rock powder experiment is important for capturing soil changes. More research is needed to understand the roles of different types of rock powders on the microbiome and how microorganisms affect the bioweathering of minerals. We hope this study will contribute to that end.

Conclusion

Different silicate rock powders caused specific changes in the SBC. At the end of the 8 months (8M), the SBCs clustered according to the rock SiO_2 content (acid rock: granite; intermediate rock: phonolite; and basic rocks: three types of basalts). In addition, variations in mineralogy, chemistry, texture and structure among the basalts led to smaller changes, causing the SBC of Ph to approach the SBC of B3, since both had zeolites, which are very reactive minerals. The SBC in the Gr treatment significantly differed from that in all the other rock powder treatments. In contrast to the rock-amended soils, the SBC in KCl showed rapid and ephemeral changes, manifested not only in the NMDS but also in the richness and Shannon indices. This was the only treatment that had a significant change after the first month (1M), and after eight months (8M), it approached C (control), while the rock-amended treatments could still be differentiated from C. The results indicate that the duration of the experiment is an important factor in rock powder management, and thorough analyses of the rock powder and soil used are essential for understanding the various possible changes in the soil–plant–water system.

Ultimately, our research highlights the importance of multiple long-term analyses in microbial geochemistry studies. This study illustrates the challenge of modeling nutrient release, and by extention the carbon dioxide removal (CDR) by enhanced rock weathering (ERW), because rock weathering and the changes in the soil microbiome need to be considered concurrently. This trial also exemplifies the potential of further advanced multidisciplinary studies focusing on the mineral and biological changes that occur simultaneously when rock powder is applied to soils. In this regard, further studies using next-generation sequencing should be valuable.

Abbreviations

CDR	Carbon dioxide removal
ERW	Enhanced rock weathering
SBC	Soil bacterial community
VFS	Very fine sand
MS	Medium sand
VCS	Very coarse sand
C	Control
Ph	Phonolite
B1	Basalt 1
B2	Basalt 2
B3	Basalt 3
Gr	Granite
EU	Experimental unit
1M	1 Month
4M	4 Months
8M	8 Months
DTPA	Diethylenetriaminepentaacetic acid
XRD	X-ray diffractometer
T-RFLP	Terminal restriction fragment length polymorphism
TRFs	Terminal restriction fragments
EC	Electrical conductivity
NMDS	Nonmetric multidimensional scaling
RDA	Redundancy analysis
SEM	Structural equation model
CFI	Comparative fit index
TLI	Tucker–Lewis index
CEC	Cation exchange capacity
MBC	Microbial biomass carbon

Supplementary Information

The online version contains supplementary material available at https://doi.org/10.1186/s40538-024-00586-w.

Additional file 1: Table S1. Physical and chemical soil characteristics.

Additional file 2: Table S2. Global redundancy analysis (RDA) at 8M output coupled with forward selection output showing the relationship between the bacteria community structure and total rock chemical elements input per pot. The forward selection detected the most predictive variables based on Monte Carlo permutation 999 with Bonferroni corrections.

Acknowledgements

We acknowledge the laboratory technicians (ESALQ-USP) for support during the experiments and analyses.

Author contributions

BRR, ACA and FDA conceived the original experimental design. BRR conducted the experiments. BRR and AMMS conducted the analyses. BRR, ALSV and AMMS led the interpretation of the data. All the authors contributed to the data interpretation and scientific writing.

Funding

This research was funded by CNPq (423069/2018-7). BRR acknowledges CNPq MSc. Grant 161401/2018-0, and ACA to CNPq research Grant 306636/2019-0.

Availability of data and materials

The datasets generated during the current study are included in the article/additional material, and further inquiries can be directed to the corresponding authors.

Declarations

Ethics approval and consent to participate

Not applicable.

Consent for publication

Not applicable.

Competing interests

The authors declare that they have no competing interests.

Author details

[1]Department of Soil Science, "Luiz de Queiroz" College of Agriculture, University of São Paulo, Av. Pádua Dias, 11, Piracicaba, SP 13415-900, Brazil.

Received: 9 February 2024 Accepted: 18 April 2024
Published online: 29 April 2024

References

1. Harley AD, Gilkes RJ. Factors influencing the release of plant nutrient elements from silicate rock powders: a geochemical overview. Nutr Cycl Agroecosystems. 2000;56:11–36.
2. van Straaten P. AGROGEOLOGY: the use of rocks for crops. Cambridge: Enviroquest Ltd.; 2007.
3. Manning DAC, Theodoro SH. Enabling food security through use of local rocks and minerals. Extr Ind Soc. 2020;7:480–7.

4. Swoboda P, Döring TF, Hamer M. Remineralizing soils? The agricultural usage of silicate rock powders: a review. Sci Total Environ. 2022;807: 150976.
5. Samuels T, Bryce C, Landenmark H, Marie-Loudon C, Nicholson N, Stevens AH, et al. Microbial Weathering of Minerals and Rocks in Natural Environments. In: John Wiley & Sons I, editor. Biogeochem Cycles Ecol Drivers Environ Impact. 1st ed. 2020. p. 59–79.
6. Flemming HC, Wuertz S. Bacteria and archaea on Earth and their abundance in biofilms. Nat Rev Microbiol. 2019;17:247–60.
7. Uroz S, Calvaruso C, Turpault MP, Frey-Klett P. Mineral weathering by bacteria: ecology, actors and mechanisms. Trends Microbiol. 2009;17:378–87.
8. Dong H, Huang L, Zhao L, Zeng Q, Liu X, Sheng Y, et al. A critical review of mineral–microbe interaction and co-evolution: mechanisms and applications. Natl Sci Rev. 2022;9: nwac128.
9. Almeida IT, Eston SM, de Assunção JV. Characterization of suspended particulate matter in mining areas in São Paulo, Brazil. Int J Surf Mining, Reclam Environ. 2002;16:171–9.
10. Novaes RML, Tubiello FN, Garofalo DFT, De Santis G, Pazianotto RAA, Folegatti-Matsuura MIDS. Brazil's agricultural land, cropping frequency and second crop area: FAOSTAT statistics and new estimates. 93rd ed. Jaguariúna: Boletim de Pesquisa e Desenvolvimento / Embrapa Environment; 2022.
11. Strefler J, Amann T, Bauer N, Kriegler E, Hartmann J. Potential and costs of carbon dioxide removal by enhanced weathering of rocks. Environ Res Lett. 2018;13: 034010.
12. Ramos CG, Hower JC, Blanco E, Oliveira MLS, Theodoro SH. Possibilities of using silicate rock powder: an overview. Geosci Front. 2022;13: 101185.
13. Lefebvre D, Goglio P, Williams A, Manning DAC, de Azevedo AC, Bergmann M, et al. Assessing the potential of soil carbonation and enhanced weathering through Life Cycle Assessment: a case study for Sao Paulo State. Brazil J Clean Prod. 2019;233:468–81.
14. Korchagin J, Caner L, Bortoluzzi EC. Variability of amethyst mining waste: a mineralogical and geochemical approach to evaluate the potential use in agriculture. J Clean Prod. 2019;210:749–58.
15. Dalmora AC, Ramos CG, Plata LG, da Costa ML, Kautzmann RM, Oliveira LFS. Understanding the mobility of potential nutrients in rock mining by-products: an opportunity for more sustainable agriculture and mining. Sci Total Environ. 2020;710: 136240.
16. USDA. Keys to Soil Taxonomy. 12th ed. Nat. Resour. Conserv. Serv. Washington, DC, USA; 2014. http://www.nrcs.usda.gov/Internet/FSE_DOCUMENTS/nrcs142p2_051546.pdf
17. IUSS Working Group WRB. World Reference Base for Soil Resources. International soil classification system for naming soils and creating legends for soil maps. 4th ed. International Union of Soil Sciences (IUSS), editor. Int. Union Soil Sci. Vienna, Austria; 2022.
18. Embrapa. Sistema brasileiro de classificação de solos. 5th ed. Empres. Bras. Pesqui. Agropecuária - Embrapa Solos. Brasília, DF; 2018.
19. Alvares CA, Stape JL, Sentelhas PC, de Moraes Gonçalves JL, Sparovek G. Köppen's climate classification map for Brazil. Meteorol Zeitschrift. 2013;22:711–28.
20. Peate DW. The Parana-Etendeka Province. In: Mahoney JJ, Coffin MF, editors. Large Igneous Prov Cont Ocean Planet Flood Volcanism. Geophysica. American Geophysical Union; 1997. p. 217–45.
21. Novais RF de, Neves JCL, Barros NF de. Ensaio em ambiente controlado. Métodos Pesqui. em Fertil. do solo. Brasília, DF: Embrapa; 1991.
22. Embrapa. Manual De Métodos de Análise de Solo. 3rd ed. Teixeira PC, Donagemma GK, Fontana A, Teixeira WG, editors. Embrapa; 2018. http://www.cse.edu.uy/sites/www.cse.edu.uy/files/documentos/Liccom_Camejo_2011-07-28.pdf
23. de Gimenes FMA, da Silva SC, Fialho CA, Gomes MB, Berndt A, Gerdes L, et al. Ganho de peso e produtividade animal em capim-marandu sob pastejo rotativo e adubação nitrogenada. Pesqui Agropecu Bras. 2011;46:751–9.
24. De Camargo OA, Moniz AC, Jorge JA, Valadares JMAS. Métodos de Análise Química, Mineralógica e Física de Solos do Instituto Agronômico de Campinas. Boletim técnico, 106. Campinas; 2009.
25. Putz H, Brandenburg K. Match! – Phase Analysis using Powder Diffraction – Version 3 [Internet]. Cryst. Impact. 2003. https://www.crystalimpact.de/match. Accessed 4 Nov 2022.
26. Gražulis S, Chateigner D, Downs RT, Yokochi AFT, Quirós M, Lutterotti L, et al. Crystallography Open Database – an open-access collection of crystal structures. Appl Crystallogr. 2009;42:726–9.
27. Chen P-Y. Table of key lines in X-ray Powder Diffraction Patterns of Minerals in Clays and Associated Rocks. Geological. Bloomington, Indiana: Department of Natural Resources; 1977.
28. Brindley GW, Brown G. Crystal structures of clay minerals and their X-ray identification. 1st ed. London: Mineralogical Society of Great Britain and Ireland; 1980.
29. Vance ED, Brookes PC, Jenkinson DS. An extraction method for measuring soil microbial biomass C. Soil Biol Biochem. 1987;19:703–7.
30. Tabatabai MA, et al. Methods of soil analysis. Microbiological and biochemical properties. In: Weaver RW, Angle S, Bottomley P, Bezdicek D, Smith S, Tabatabai A, et al., editors. Soil. Sci. Soc. Am. B. Ser. Madison: Soil Science Society of America; 1994.
31. Schütte UME, Abdo Z, Bent SJ, Williams CJ, Schneider GM, Solheim B, et al. Bacterial succession in a glacier foreland of the High Arctic. ISME J. 2009;3:1258–68.
32. Durrer A, Gumiere T, Taketani RG, da Costa DP, de Pereira e Silva MC, Andreote FD. The drivers underlying biogeographical patterns of bacterial communities in soils under sugarcane cultivation. Appl Soil Ecol. 2017;110:12–20.
33. Pimentel LG, Gumiere T, Oliveira DMS, Cherubin MR, Andreote FD, Cerri CEP, et al. Soil bacterial community changes in sugarcane fields under straw removal in Brazil. Bioenergy Res. 2019;12:830–42.
34. Ercolini D, Cocolin L. Identification Methods | Culture-Independent Techniques. In: Batt CA, Tortorello MLBT-E of FM (Second E, editors. Encycl Food Microbiol. Second Ed. Oxford: Academic Press; 2014. p. 259–66.
35. Nguyen NH, Song Z, Bates ST, Branco S, Tedersoo L, Menke J, et al. FUNGuild: an open annotation tool for parsing fungal community datasets by ecological guild. Fungal Ecol. 2016;20:241–8.
36. Dickie IA, FitzJohn RG. Using terminal restriction fragment length polymorphism (T-RFLP) to identify mycorrhizal fungi: a methods review. Mycorrhiza. 2007;17:259–70.
37. De Vrieze J, Ijaz UZ, Saunders AM, Theuerl S. Terminal restriction fragment length polymorphism is an "old school" reliable technique for swift microbial community screening in anaerobic digestion. Sci Rep. 2018;8:16818.
38. Schütte UME, Abdo Z, Bent SJ, Shyu C, Williams CJ, Pierson JD, et al. Advances in the use of terminal restriction fragment length polymorphism (T-RFLP) analysis of 16S rRNA genes to characterize microbial communities. Appl Microbiol Biotechnol. 2008;80:365–80. https://doi.org/10.1007/s00253-008-1565-4.
39. Aiken JT. Terminal restriction fragment length polymorphism for soil microbial community fingerprinting. Soil Sci Soc Am J. 2011;75:102–11. https://doi.org/10.2136/sssaj2008.0088.
40. Lindström S, Rowe O, Timonen S, Sundström L, Johansson H. Trends in bacterial and fungal communities in ant nests observed with Terminal-Restriction Fragment Length Polymorphism (T-RFLP) and Next Generation Sequencing (NGS) techniques—validity and compatibility in ecological studies. PeerJ. 2018;6: e5289. https://doi.org/10.7717/peerj.5289.
41. Laxen DPH, Harrison RM. A scheme for the physico-chemical speciation of trace metals in freshwater samples. Sci Total Environ. 1981;19:59–82.
42. Araújo GCL, Gonzalez MH, Ferreira AG, Nogueira ARA, Nóbrega JA. Effect of acid concentration on closed-vessel microwave-assisted digestion of plant materials. Spectrochim Acta Part B At Spectrosc. 2002;57:2121–32.
43. Zhang R, Thiyagarajan V, Qian P-Y. Evaluation of terminal-restriction fragment length polymorphism analysis in contrasting marine environments. FEMS Microbiol Ecol. 2008;65:169–78.
44. Blackwood CB, Hudleston D, Zak DR, Buyer JS. Interpreting ecological diversity indices applied to terminal restriction fragment length polymorphism data: insights from simulated microbial communities. Appl Environ Microbiol. 2007;73:5276–83.
45. Ramette A. Multivariate analyses in microbial ecology. FEMS Microbiol Ecol. 2007;62:142–60.
46. Oksanen J, Kindt R, Legendre P, O'Hara B, Simpson GL, Solymos PM, et al. The vegan package. Community Ecol. Packag. 2008. p. 190. http://cran.r-project.org/, http://vegan.r-forge.r-project.org/

47. de Vries FT, Griffiths RI, Bailey M, Craig H, Girlanda M, Gweon HS, et al. Soil bacterial networks are less stable under drought than fungal networks. Nat Commun. 2018;9:3033.
48. Yang L, Wang N, Chen Y, Yang W, Tian D, Zhang C, et al. Carbon management practices regulate soil bacterial communities in response to nitrogen addition in a pine forest. Plant Soil. 2020;452:137–51.
49. de Lopes BAB, Silva AMM, Santana MC, Feiler HP, de Pereira APA, Teixeira MF, et al. Arbuscular mycorrhizal fungi and soil quality indicators in eucalyptus genotypes with different drought tolerance levels. Front Fungal Biol. 2022. https://doi.org/10.3389/ffunb.2022.913570.
50. Rosseel Y. lavaan: an r package for structural equation modeling. J Stat Softw. 2012;48:1–36.
51. Epskamp S. semplot: unified visualizations of structural equation models. Struct Equ Model A Multidiscip J. 2015;22:474–83.
52. Streckeisen A. Classification and nomenclature of volcanic rocks, lamprophyres, carbonatites and melilitic rocks IUGS Subcommission on the Systematics of Igneous Rocks - recommendations and suggestions. Geol Rundschau. 1980;69:194–207.
53. Cui X, Zhang Y, Gao J, Peng F, Gao P. Long-term combined application of manure and chemical fertilizer sustained higher nutrient status and rhizospheric bacterial diversity in reddish paddy soil of Central South China. Sci Rep. 2018;8:1–11.
54. Liang R, Hou R, Li J, Lyu Y, Hang S, Gong H, et al. Effects of different fertilizers on rhizosphere bacterial communities of winter wheat in the North China Plain. Agronomy. 2020;10:93.
55. Allison SD, Martiny JBH. Resistance, resilience, and redundancy in microbial communities. Proc Natl Acad Sci U S A. 2008;105:11512–9.
56. Zhang Y, Hao X, Garcia-Lemos AM, Nunes I, Nicolaisen MH, Nybroe O. Soil fertilization has different effects on bacterial community composition in the Penicillium canescens hyphosphere and in bulk soil. Appl Environ Microbiol. 2020. https://doi.org/10.1128/AEM.02969-19.
57. Ben Zineb A, Trabelsi D, Barhoumi F, Dhane SF, Mhamdi R. Potentialities and soil impact analysis of rock phosphorus fertilization of perennial and annual legume crops. Arch Agron Soil Sci. 2019;66:1074–88.
58. Epstein W. The roles and regulation of potassium in bacteria. Prog Nucleic Acid Res Mol Biol. 2003;75:293–320.
59. Lester G. Requirement for potassium by bacteria. J Bacteriol. 1958;75:426–8.
60. Essington ME. Soil and Water Chemistry An Integrative Approach. In: Soil Water Chem. 1st ed. Boca Raton: CRC Press; 2003.
61. Friedman R. Membrane-ion interactions. J Membr Biol. 2018;251:453–60.
62. Halverson LJ. Bacteria in Soil. Ref Modul Earth Syst Environ Sci. Iowa State University, Ames, IA, USA: Elsevier Inc.; 2014.
63. Xia Z, Bai E, Wang Q, Gao D, Zhou J, Jiang P, et al. Biogeographic distribution patterns of bacteria in typical chinese forest soils. Front Microbiol. 2016;7:1106.
64. Lacroix E, Brovelli A, Barry DA, Holliger C. Use of silicate minerals for pH control during reductive dechlorination of chloroethenes in batch cultures of different microbial consortia. Appl Environ Microbiol. 2014;80:3858–67.
65. Lacroix E, Brovelli A, Holliger C, Barry DA. Evaluation of silicate minerals for pH control during bioremediation: application to chlorinated solvents. Water Air Soil Pollut. 2012;223:2663–84.
66. Lacroix E, Brovelli A, Holliger C, Barry DA. Control of groundwater pH during bioremediation: improvement and validation of a geochemical model to assess the buffering potential of ground silicate minerals. J Contam Hydrol. 2014;160:21–9.
67. Čuhel J, Malý S, Královec J. Shifts and recovery of soil microbial communities in a 40-year field trial under mineral fertilization. Pedobiologia (Jena). 2019;77: 150575.
68. Mickan BS, Alsharmani AR, Solaiman ZM, Leopold M, Abbott LK. Plant-dependent soil bacterial responses following amendment with a multi-species microbial biostimulant compared to rock mineral and chemical fertilizers. Front Plant Sci. 2021;11: 550169.
69. Li J, Mavrodi DV, Dong Y. Effect of rock dust-amended compost on the soil properties, soil microbial activity, and fruit production in an apple orchard from the Jiangsu province of China. Arch Agron Soil Sci. 2020;67:1313–26.
70. de Lopes AAC, de Sousa DMG, Chaer GM, dos Junior FBR, Goedert WJ, de Mendes IC. Interpretation of microbial soil indicators as a function of crop yield and organic carbon. Soil Sci Soc Am J. 2013;77:461–72.
71. Castro Lopes AA, Sousa DMG, dos Reis FB, Figueiredo CC, Malaquias JV, Souza LM, et al. Temporal variation and critical limits of microbial indicators in oxisols in the Cerrado, Brazil. Geoderma Reg. 2018;12:72–82.
72. De Barros JA, De Medeiros EV, Da Costa DP, Duda GP, De Sousa Lima JR, Dos Santos UJ, et al. Human disturbance affects enzyme activity, microbial biomass and organic carbon in tropical dry sub-humid pasture and forest soils. Arch Agron Soil Sci. 2019;66:458–72.
73. Mirzavand J, Asadi-Rahmani H, Moradi-Talebbeigi R. Biological indicators of soil quality under conventional, reduced, and no-tillage systems. Arch Agron Soil Sci. 2020;68:311–24.
74. Rodrigues RN, Junior FBDR, de Lopes AAC, Rocha OC, Guerra AF, Veiga AD, et al. Soil enzymatic activity under coffee cultivation with different water regimes associated to liming and intercropped brachiaria. Ciência Rural. 2021;52:3.
75. Vinhal-Freitas IC, Corrêa GF, Wendling B, Bobuľská L, Ferreira AS. Soil textural class plays a major role in evaluating the effects of land use on soil quality indicators. Ecol Indic. 2017;74:182–90.
76. Janes-Bassett V, Blackwell MSA, Blair G, Davies J, Haygarth PM, Mezeli MM, et al. A meta-analysis of phosphatase activity in agricultural settings in response to phosphorus deficiency. Soil Biol Biochem. 2022;165: 108537.
77. de Richter DB, Oh N-H, Fimmen R, Jackson J. The rhizosphere and soil formation. In: Cardon ZG, Whitbeck JL, editors. Rhizosph - an ecol perspect. Cambridge: Academic Press; 2007. p. 179–200.

Publisher's Note